Plasma-enhanced growth, composition, and refractive index of silicon oxy-nitride films

Mattsson, Kent Erik

Published in:
Journal of Applied Physics

Link to article, DOI:
10.1063/1.359072

Publication date:
1995

Document Version
Publisher's PDF, also known as Version of record

Plasma-enhanced growth, composition, and refractive index of silicon oxy-nitride films

Kent Erik Mattsson
NKT Research Center A/S, Sognevej 11, Dk-2605 Brøndby, and MikroelektronikCentret, Technical University of Denmark, Bldg. 345 Ø, Dk-2800 Lyngby, Denmark

(Received 20 September 1994; accepted for publication 15 February 1995)

Secondary ion mass spectrometry and refractive index measurements have been carried out on silicon oxy-nitride produced by plasma-enhanced chemical vapor deposition (PECVD). Nitrous oxide and ammonia were added to a constant flow of 2% silane in nitrogen, to produce oxy-nitride films with atomic nitrogen concentrations between 2 and 10 at. %. A simple atomic valence model is found to describe both the measured atomic concentrations and published material compositions for silicon oxy-nitride produced by PECVD. A relation between the Si–N bond concentration and the refractive index is found. This relation suggest that the refractive index of oxy-nitride with a low nitrogen concentration is determined by the material density. It is suggested that the relative oxygen concentration in the gas flow is the major deposition characterization parameter, and that water vapor is the predominant reaction by-product. A model, that combine the chemical net reaction and the stoichiometric rules, is found to agree with measured deposition rates for given material compositions. Effects of annealing in a nitrogen atmosphere has been investigated for the 400 °C–1100 °C temperature range. It is observed that PECVD oxy-nitrides release nitrogen and hydrogen in the form of NH for annealing temperatures in the 500 °C–700 °C range. The relaxation process during annealing is found to be governed by a viscoelastic relaxation process similar to the relaxation process observed for thermally grown SiO_2. Upon nitrogen release, the PECVD material is in a state of internal tension. The viscoelastic relaxation process for temperatures above 700 °C is dominated by the relaxation of this internal tension. A linear relation between the refractive index and material density is determined for silicon oxy-nitride with a nitrogen concentration below 30 at. %. © *1995 American Institute of Physics.*

I. INTRODUCTION

Silicon oxy-nitride films grown by plasma enhanced chemical vapor deposition (PECVD) are widely used as interlayer insulation or passivation for integrated electrical circuit and solar cell technologies,[1–5] Further, silicon oxy-nitride has found application as core layer material in integrated optical circuit technology.[6–8]

Extensive work has been done to characterize amorphous hydrogenated silicon oxy-nitride, usually deposited with nitrous oxide as the oxygen source, with ammonia as the nitrogen source and with silane as the silicon source. This work has been applied to the hydrogen chemistry, growth mechanisms, and mechanical characteristics of PECVD silicon oxynitride.[1–5,9–11] Most of the work on the thermal stability of amorphous hydrogenated silicon oxy-nitride has been applied to the electrical properties, hydrogen chemistry, mechanical stress and viscoelastic relaxation processes.[12–17]

In the first part of this paper a study of the influence of material composition on the refractive index of *as deposited* silicon oxy-nitride with low concentrations of nitrogen (0–10 at. %) will be presented. In the second part of this paper effects of annealing on silicon oxy-nitride are investigated. The material is investigated as a possible candidate for core material in integrated optical waveguides. The design of optical waveguides with controlled mode size requires that the refractive indices of the dielectric films are accurately known. For example a waveguide that is well matched to the mode of a standard single-mode optical transmission fiber, will have a core cladding difference in refractive index of $\sim 6 \cdot 10^{-3}$. Further, a low level of light reflected back into the optical fiber will require the absolute value of the refractive index to be close to the refractive index of the fiber glass (within $\sim 10^{-2}$). Thus it is desirable to control the refractive indices of the dielectric films with an accuracy of a few times 10^{-4}.

The refractive index of the dielectric films are measured with a prism coupler to an accuracy of $\sim 2 \cdot 10^{-4}$ at a wavelength of 632.8 nm. The elemental composition of the deposited films are measured by secondary ion mass spectrometry (SIMS). The relative concentrations are determined to an accuracy of ~ 2 % for the silicon, oxygen, nitrogen and hydrogen composition.

The established compositions suggest that the material is deposited in a "stoichiometric" form which can be modeled. The individual components act in accordance with their accepted fixed valencies. The model for the material is based on the valence bond theory and Pauling's rules.[18] This model is shown to fit with compositions for silicon oxy-nitride determined by other research groups. Based on the model is it suggested that the nitrogen concentration for the deposition of silicon oxy-nitride is determined by the relative concentration of nitrogen and oxygen in the gas mixture. With a high relative concentration of oxygen the dominant by-product in the film formation is expected to be water vapor.

The hydrogen-contents of PECVD deposited films is relatively high. This may result in film-material with nondesired optical absorption bands. The hydrogen content may be

 0021-8979/95/77(12)/6616/8/$6.00

reduced by annealing. Since the application in mind is integrated optics the focus of the study in the second part of this paper is the refractive index, thickness change, internal stress relaxation and material composition as function of annealing temperature. The measures of these suggest that the PECVD material releases nitrogen and hydrogen during annealing. Most of the nitrogen is released at annealing temperatures in the 500 °C–700 °C range.

For silicon dioxide material is it observed that equal amounts of nitrogen and hydrogen are released upon annealing. This reduction is believed to be due to the release of nitrogen and hydrogen from the glass matrix in the form of NH. This release does not necessarily include a breaking of the N–H bond, and is in accordance with the findings of Mulfinger.[19] Here glass which has dissolved nitrogen under reducing conditions is found to release nitrogen under oxidizing and weakly reducing ambients.

The annealing behavior at temperatures above 600 °C depends on the actual deposition process parameters (i.e., gas composition and discharge power). It is found that the porosity and internal tension which follows the release of nitrogen is reduced for material deposited with higher deposition power densities. This is believed to be due to a reduced concentration of nitrogen and hydrogen in the deposited material.

II. EXPERIMENTS

A. Deposition

Silicon oxy-nitride material with low nitrogen concentration is grown, to obtain core glass material that exhibits a refractive index slightly higher than silicon dioxide, i.e., fits to the refractive index of an optical fiber.

A load-locked parallel-plate reactor operating at 380 kHz and 0.4 Torr was used for the deposition of the silicon oxy-nitride films. The rf power density was 0.75 W/cm^2. The films were deposited on one side of the wafers at 300 °C with varying flows of nitrous oxide and ammonia to a constant flow of 850 sccm of 2% silane in nitrogen. The sum of the nitrous oxide and ammonia flows were kept constant at a flow of 1700 sccm. The substrates were 100-mm diameter, (100), *n*-type Si wafers.

For the annealing experiments silicon oxy-nitride films were grown at 300 °C and 0.7 Torr. Two types of processes were used. The first process (type-I) aimed at the fabrication of buffer glass, i.e., pure silicon dioxide. This process used silane and nitrous oxide in a ratio of 1:100. The second process (type-II) was a core glass process, i.e., silicon oxy-nitride with low nitrogen concentration. A gas mixture of silane, nitrous oxide and ammonia was used in a ratio of 1: 94:6. Both types of processes were performed with rf discharge power densities of 0.5, 0.75, 0.9, 1.0, and 1.5 W/cm^2, respectively.

The annealing of the samples was performed in a nitrogen atmosphere in a standard oxidation furnace. The post-deposition thermal processing was carried out at annealing temperatures ranging from 250 °C to 1100 °C for 30 min at each temperature.

A second batch with identical process parameters was produced for SIMS measurements. The wafers of this batch were broken into four pieces and annealed in a nitrogen atmosphere at 300, 600, 800, and 1100 °C, respectively, for 30 min.

B. Analysis

Layer thickness and refractive indices are measured using a prism coupler at a wavelength of 632.8 nm. The refractive index is determined with an accuracy better than $\pm 2 \cdot 10^{-4}$ and the thickness to better than ± 0.01 μm. The effective deposition rates are determined from the measured layer thickness divided by the plasma-on time.

The mechanical stress of the deposited layers is determined at room temperature by measuring the curvature of the wafers with a stylus force gauge. The wafers were scanned before annealing to determine the initial warpage of the wafer with deposited film. These scans were subtracted from the scans obtained at the same positions upon annealing to determine the change in film stress. In this manner the mechanical stress of the deposited layers is determined to an accuracy of ± 10 MPa.

The material composition is measured by SIMS. A primary 2.5 keV Cs^+ ion beam is used as sputter source and secondary negative ions are extracted. The material composition is determined by mass separation of the secondary ions. The sample intercept the primary Cs^+ beam at an angle of 70° from normal. The surface is charge compensated by an electron beam which makes it possible to measure even when the sample is made of insulating material.

The absolute concentration of nitrogen and hydrogen are determined relative to calibration samples produced by ion implantation. The ions are implanted into thermal oxide which simultaneously acts as a reference for the silicon and oxygen concentrations.

The nitrogen concentration is obtained from the mass-42 line (SiN^-) relative to a reference sample which is measured in the same run. The oxygen concentration is determined from the sputter rate and mass-42 to mass-44 (SiO^-) ratio. The silicon is in a similar manner determined from the mass-56 (Si_2^-) to mass-44 ratio. The hydrogen concentration is determined from the mismatch in counts between the mass-42, mass-43 ($HSiN^-$) and mass-44, mass-45 ($HSiO^-$) lines, respectively. The mass-42 corresponds to the Si_{28}-N_{14}^- ion, whereas mass-43 gives both Si_{29}-N_{14}^- and Si_{28}-N_{14}-H^- ions. With the measure for mass-42 and from the natural abundance of silicon, the concentration of hydrogen is determined. The present configuration of the SIMS equipment does not allow for a direct mass-1 analysis.

The absolute concentration of nitrogen and hydrogen is experienced to vary with ~7%, due to an unstable surface charge compensation and corresponding ion production. The annealing of silicon oxy-nitride caused the hydrogen concentration to sink below the detection limit of the SIMS system. This detection limit is primarily determined by the base pressure in the UHV chamber. For a pressure of $6 \cdot 10^{-10}$ Torr the detection limit for hydrogen is $\sim 1 \cdot 10^{20}$ cm^{-3}, which corresponds to an atomic concentration of ~0.2 at. %. The detec-

TABLE I. Deposition parameters and measured refractive index, composition and deposition rate.

Sample #	NH_3:N_2O (sccm)	Composition Si	O	N	H	Density (g/cm^3)	Index (6328 Å)	Rate (Å/min)
526	0:1700	32.5	63.4	1.8	2.2	2.26±0.14	1.4700	2055
527	100:1600	32.1	60.9	3.4	3.5	2.31±0.17	1.4808	1952
528	150:1550	31.9	56.7	6.3	5.1	2.35±0.16	1.4887	1813

tion limit for nitrogen was found to be $\sim 2 \cdot 10^{18}$ cm^{-3}, which corresponds to an atomic concentration of ~30 ppm. This is determined by measurement from the area below the nitrogen implantation profile in a thermal oxide. The measured concentrations are corrected for the background of counts from the chamber. Hereby, a measure for the relative concentration of nitrogen, hydrogen, oxygen and silicon can be obtained from the mass line ratios 42 : 44, "43" : 42 and 44 : 56, respectively. It is experienced that even though the absolute concentration of nitrogen and hydrogen varies, for a sample measured in various runs, the ratios between the various mass lines are stable. The relative concentrations are determined by use of the mass line ratios to an accuracy level of ~2 % of their relative size.

III. AS DEPOSITED MATERIAL

A. Experimental results

The elemental composition of the *as deposited* films determined by SIMS, the measured refractive index, and the effective deposition rates are presented in Table I. The elemental composition data is average values based on three runs of the same samples. It was found that the material composition and concentration was constant as function of depth as characterized by SIMS. The increase in ammonia flow can be observed to cause an increase in nitrogen and hydrogen atomic percent, and a decrease in oxygen. The silicon atomic percent is unchanged (within the accuracy limit).

The material density is estimated from the average values of the individual compositions. As can be observed, the density of the material increases with increasing ammonia content in the gas mix. The large standard deviation on the estimated densities is due to the large spread in measured nitrogen concentration.

The refractive index increases with increasing ammonia concentration whereas the deposition rate decrease with increasing ammonia concentration in the deposition gas mixture.

B. Material composition

From the accepted main valencies of silicon (+4), oxygen (-2) and nitrogen (-3), a stoichiometric composition of silicon oxy-nitride can be predicted. Under the assumption that the sum of the positive vacancies must equal that of the negative ones, it is obtained:

$$X_O = \tfrac{2}{3} - \tfrac{7}{6} X_N \quad (1)$$

$$X_{Si} = \tfrac{1}{3} + \tfrac{1}{6} X_N \quad (2)$$

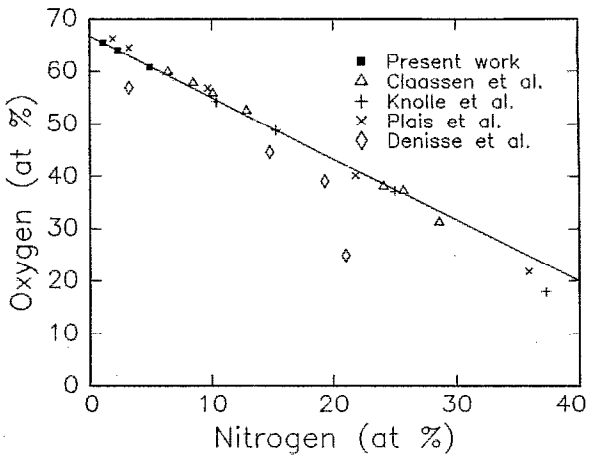

FIG. 1. "Active" oxygen concentration as function of "active" nitrogen concentration. The solid line represents stoichiometric material.

where X_{Si}, X_O and X_N represent the atomic percent of silicon, oxygen and nitrogen, respectively.

The relations in Eqs. (1) and (2) state that with increasing nitrogen concentration in the silicon oxy-nitride, the oxygen concentration will decrease and the silicon concentration will increase.

The curves obtained from Eqs. (1) and (2) for stoichiometric silicon oxy-nitride are shown in Figs. 1 and 2, respectively, along with published data.[1,3-5] The "active" concentrations for the published data are observed to fit well to the stoichiometric model. The data material is obtained from different equipment with various deposition conditions. This suggests that a general set of stoichiometric rules governs the formation of silicon oxy-nitride.

The term "active" indicates that the number of hydrogen related bonds has been subtracted the actual atomic composition (i.e., hydrogen bond to silicon requires $\frac{1}{4}$ silicon atom, bond to oxygen requires $\frac{1}{2}$ oxygen atom, and bond to nitrogen require $\frac{1}{3}$ nitrogen atom). The remaining concentrations is

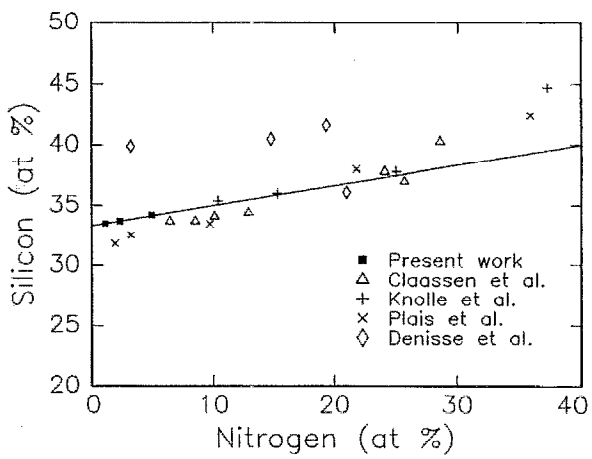

FIG. 2. "Active" silicon concentration as function of "active" nitrogen concentration. The solid line represents stoichiometric material.

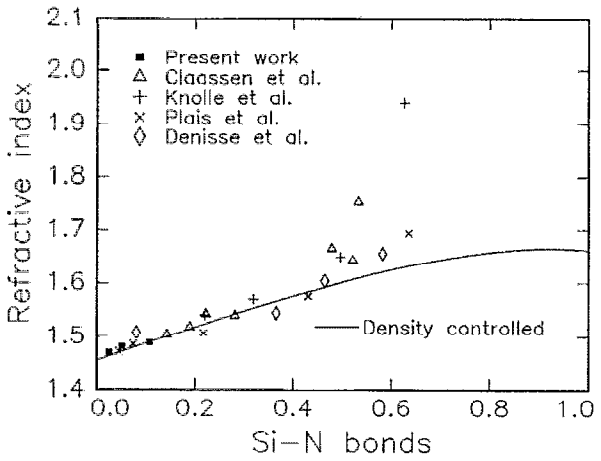

FIG. 3. Refractive index as function of relative number of Si–N bonds. The solid line is the silicon dioxide density controlled refractive index.

then rescaled and plotted against the active nitrogen concentration.

It is observed by several research groups that for oxynitride with low nitrogen concentration the hydrogen is dominantly bond to nitrogen whereas the amount of hydrogen bond to silicon is small.[1,3,4]

The measured concentration of Si–H, N–H and O–H bond is applied in Figs. 1 and 2. The "active" oxygen and silicon atomic percent is shown as function of the "active" nitrogen atomic percent from the present work and from published data.[1,3–5] For the data by Plais *et al.*[5] is it assumed that the hydrogen is bond to oxygen rather than nitrogen or silicon. In oxygen rich films it is generally observed that the hydrogen is to be found in a O–H bond.[12] All other data apply the measured Si–H and N–H bond concentrations with estimates on the mass density from the refractive index, as will be discussed in the following section.

The material reported by Denisse *et al.* is found to deviate somewhat from the stoichiometry. This deviation indicates that direct Si–Si bonds are present in the material. An explanation for this might be obtained from the observations made by Nguyen,[9] where the initial transient phenomenon in plasma processing is associated with the formation of films with low hydrogen content and high silicon content. The silicon rich films by Denisse *et al.* are deposited in the limited depletion mode, where the rf field is pulsed with a frequency of 4 Hz and a pulse width of about 100 ms. This might lead to a process where the plasma never leaves the initial transient state, which could account for the silicon rich films obtained.

C. Refractive index

The refractive index of the samples measured with a prism coupler is shown in Fig. 3 as function of the relative number of Si–N bonds. This number is obtained from the estimated "active" concentrations of silicon and nitrogen. Data from Claassen *et al.*,[3] Knolle *et al.*,[4] Plais *et al.*,[5] and Denisse *et al.*[1] are shown for comparison, along with the expected refractive index of densified glass from Sec. IV C.

As can be observed, the measured refractive index and the published data fit well with the mass density curve for a relative number of Si–N bonds below 0.4. Above 0.4, all the refractive indices are observed to deviate from the mass density curve, and the data seem to part into two different regimes.

For a relative number of Si–N bonds below 0.4, the refractive index is controlled by the specific volume of oxygen, i.e., the density of electrons in Si–O bonds. The position of the infrared vibrational absorption band at 1080 cm^{-1} (asymmetric vibrational Si–O–Si bond) can in the data by Budhani *et al.*[20] be observed to move slightly towards lower wavenumbers for material with increasing nitrogen concentrations. This indicates that the bond angle of the Si–O–Si bridges decreases slightly, in accordance with an increase in the mass density.

For a relative Si–N bond number above 0.6 the stoichiometric model suggests that the material density of silicon nitride is reached. This can be observed from the saturation of the density curve in Fig. 3. The excess increase in refractive index observed for relative Si–N bond number above 0.4–0.5 is believed to be due to a large shift in the position of the ultraviolet absorption edge towards smaller wavenumbers. Such a shift in both the ultraviolet and infrared absorption edge has been observed by Hampshire *et al.*[21]

The shift in the ultraviolet and infrared absorption edge can be associated with a shift in bond strength of the electrons and bond angle of the atoms from an oxygen to a nitrogen dominated type. The material is with increasing nitrogen concentration transformed from a silicon dioxide dominated network to a silicon nitride dominated network. The nitrogen dominated material is less flexible than the oxygen dominated material, mainly due to the higher cross linkage of the glass matrix, which results in a more rigid glass network.

The refractive index data is observed to part into two different regimes for relative Si–N bond number above 0.5. The mechanical stress of the material from these two regimes can from the published data be found to be in a state of internal tension and compression, respectively.[1,3–5] This could indicate that the internal stress has a major influence on the position of the ultra-violet absorption edge. It is, however, beyond the scope of this paper to described these phenomena in further detail.

D. Deposition rate

The deposition rate is observed to decrease with increasing ammonia concentration in the deposition gas mixture. This behavior can be interpreted in terms of the net reactions suggested by Lucovsky *et al.*[11] For a sufficient activation of the gas mixture and a large concentration of oxygen, the reaction by-product of the heterogenous surface reaction is water vapor.

A large number of reaction pathways exist in the fully activated gas mixture, which may be responsible for the main part of the observed hydrogen in the as deposited material.[22] All these reactions are included in one net reaction shown in Eq. (3).

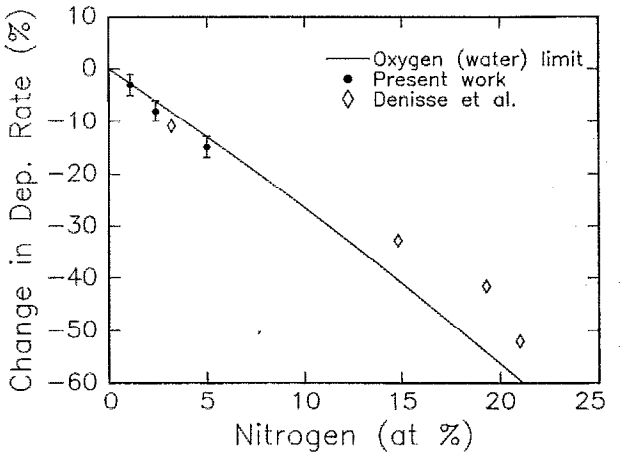

FIG. 4. Change in deposition rate as function of active nitrogen concentration. The solid line represents an oxygen limited deposition.

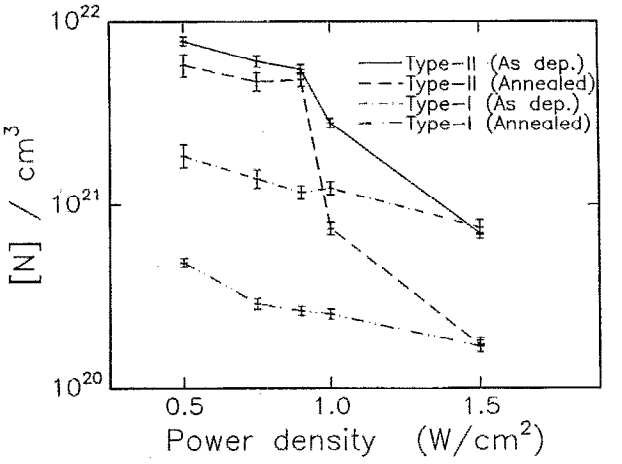

FIG. 5. Nitrogen concentration ([N]) as function of power density for core glass (type-II) and buffer glass (type-I).

$$X\ SiH_4+(2X+Y+\tfrac{3}{2}Z)\ N_2O+Z\ NH_3 \rightarrow Si_XO_YN_Z+(2X+\tfrac{3}{2}Z)\ H_2O+(2X+Y+\tfrac{3}{2}Z)\ N_2. \quad (3)$$

Under the assumption of ammonia being the dominant nitrogen source and all hydrogen being removed from the surface as water vapor, the formation of one mole $Si_XO_YN_Z$ requires $(X+\frac{1}{2}Y+\frac{3}{4}Z)$ mole O_2. Assuming that the radical production is unchanged when the ammonia concentration is increased, the relative change in deposition rate with increasing nitrogen concentration can be determined from the stoichiometric rules of Sec. III B and Eq. (3) as shown in Fig. 4. Here, the relative deposition rate is shown as function of the active nitrogen concentration. The three measured depositions are shown along with data from Denisse *et al.*[1] The first point of both series has been determined from the measured material compositions, whereas the remaining points are obtained from the measured deposition rates. Some similarity is observed between the measured points and the deposition limit determined by water vapor.

The measured deposition rates suggest that the relative oxygen concentration in the gas flow is the limiting factor of the film formation process for high deposition rates (1000–2000 Å/min). The oxygen reacts with the silane to form the silicon dioxide network and to some extent removes hydrogen in the form of water vapor from the growing surface.

The inclusion of nitrogen for material deposited from silane and nitrous oxide could be due to the presence of $\cdot Si(OH)_2(NH_2)$ precursors formed in the gas phase. The presence of $\cdot Si(OH)_3$ and $\cdot Si(OH)_2(NH_2)$ molecules in the discharge region of a parallel plate reactor system is observed by Smith and Alimonda by mass spectrometry.[23] With a silanol product as represented by $\cdot Si(OH)_2(NH_2)$ one of the film formation reaction paths can be described by the reaction:

$$(Si)_{FILM}-OH+(NH_2)\dot{S}i(OH)_2 \rightarrow (Si)_{FILM}-NH-\dot{S}i(OH)_2+H_2O \quad (4)$$

where $(Si)_{FILM}$-OH represents a OH group placed at the film surface.

Equation (4) states that the inclusion of nitrogen through a $\cdot Si(OH)_2(NH_2)$ precursor most likely will lead to equal concentrations of nitrogen and hydrogen in the as deposited material. The presence of equal amounts of nitrogen and hydrogen are observed for the samples in Table I. Also published data with low nitrogen concentration are observed to exhibit equal amounts of nitrogen and hydrogen.[1,3] This indicates that a silanol precursor might participate in the deposition process.

It has been shown by Mulfinger[19] that nitrogen can be dissolved under reducing conditions in silica melts. In the presence of a reducing agent (hydrogen or ammonia) in a nitrogen atmosphere, nitrogen is incorporated in the glass as NH-, and oxygen released in the form of water vapor. Mulfinger[19] concludes that glass which has dissolved nitrogen under reducing conditions may release nitrogen under oxidizing and weakly reducing ambients. The implications of this will be presented in connection with the annealing experiments.

IV. ANNEALING EFFECTS

A. Material composition

The nitrogen and hydrogen concentration for core glass (type-II) and buffer glass (type-I) deposited with various power densities is shown in Figs. 5 and 6, respectively. The post-anneal concentrations of nitrogen and hydrogen is for both types of glass within the uncertainty on the measurements found to be independent on the annealing temperature (for a 30 min anneal at 600 °C, 800 °C and 1100 °C, respectively).

The silicon and oxygen concentrations of the deposited material agree with the stoichiometric rules outlined in Sec. III B. For annealing temperatures above 600 °C, the silicon to oxygen ratio is conserved whereas the nitrogen and hydrogen concentrations decrease. This results in a substoichiometric silicon rich material. The stability of the hydrogenated

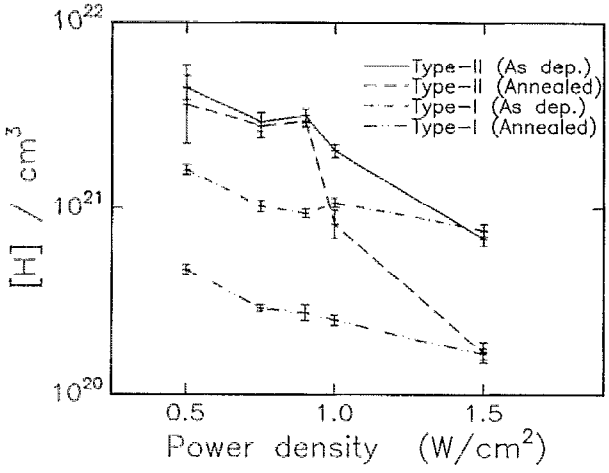

FIG. 6. Hydrogen concentration ([H]) as function of power density for core glass (type-II) and buffer glass (type-I).

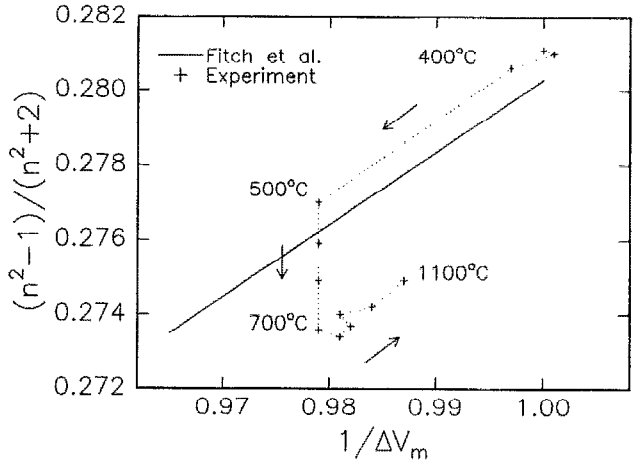

FIG. 7. Effective dielectric constant as function of fractional volume for buffer glass (type-I) deposited with a power density of 0.5 W/cm^2. The solid line represents the annealing behavior of thermal silicon dioxide dry oxidized at 850 °C.

silicon oxy-nitride depends on the deposition power density. Both the nitrogen and hydrogen concentrations decrease with increasing power density. For the core glass, a shift in the nitrogen activation is observed at a power density of 1.0 W/cm^2. At higher power densities the material approaches the nitrogen and hydrogen concentrations of buffer glass and exhibits a similar annealing behavior.

For buffer glass equal amounts of nitrogen and hydrogen are released from the material upon annealing. This suggests that nitrogen and hydrogen are released from the material as NH. For core glass produced at low power density a higher nitrogen concentration is present of which only a fraction binds to hydrogen. This results in a much smaller reduction in the nitrogen and hydrogen concentrations upon annealing. This suggests that only nitrogen bond to hydrogen is released from the material upon annealing.

The release of nitrogen presents an alternative explanation to the decomposition of N–H bonds at lower temperatures than Si–H bonds previous suggested in the literature,[12–17] for oxy-nitride with high oxygen concentration. Such a decomposition is, as also mentioned in these papers, in contradiction with the values for the respective bond energies and with the anneal behavior of plasma silicon nitride and silicon oxy-nitride with high nitrogen concentration.[12–17] The selective release of NH could account for all observations simultaneously.

B. Molar volume and mechanical stress

The changes in refractive index in thermally grown oxides can be quantitatively accounted for in terms of the Clausius–Mossotti relation[15] (also known as the Lorentz–Lorentz equation[24]). A decrease in the film density will according to equation 5 result in an increase in the molar volume, when the molar refraction and the number of atoms remains constant.

$$\frac{n^2-1}{n^2+2}\frac{M}{\rho}=\frac{n^2-1}{n^2+2}\frac{V_m}{n_m}=R; \quad R=\frac{4\pi}{3}\frac{N_A}{\epsilon_0}\alpha_e \tag{5}$$

where n, M, ρ, V_m, n_m and R are refractive index, molecular weight, density, molar volume, number of mole and molar refraction, respectively. And for the molar refraction N_A, ϵ_0, and α_e are Avogadro's number, dielectric constant of free space, and average electronic polarizability, respectively.

Since the deposited film is constrained in the plane of the substrate, changes in molar volume (density) from annealing must manifest themselves as changes in film thickness.[15] The relative molar volume change ΔV_m can be written in terms of the thickness change from annealing as

$$\Delta V_m = 1+\frac{\Delta t}{t} \tag{6}$$

where t and Δt is the deposited film thickness and the thickness change from annealing, respectively.

The refractive index and thickness change for the sample deposited with a power density of 0.5 W/cm^2 and interpreted by the Clausius–Mossotti relationship is shown in Fig. 7. The arrows indicate the path that the molar volume follows when the annealing temperature is increased. Along with the PECVD samples is shown a linear fit to data by Fitch *et al.*[15] for a thermal oxide. The linear fit is for a dry thermal oxide grown at 850 °C which is rapid thermally annealed (100 s) at 850 °C, 900 °C, 950 °C, 1000 °C, and 1100 °C.

The molar volume for the PECVD material can for annealing temperatures below 500 °C be observed to follow the Clausius–Mossotti relationship. At 500 °C a shift in the effective dielectric constant is observed without a shift in the thickness (relative molar volume). This indicates according to Equation (5) that the number of film atoms is reduced, i.e. the material density is reduced. This is in accordance with the SIMS analysis, where the initial nitrogen concentration of $1.8\cdot10^{21}$ cm^{-3} is reduced to a concentration of $4.1\cdot10^{20}$ cm^{-3} for annealing at 600 °C.

A densification takes place for annealing temperatures above 700 °C. The densification follows the slope of the

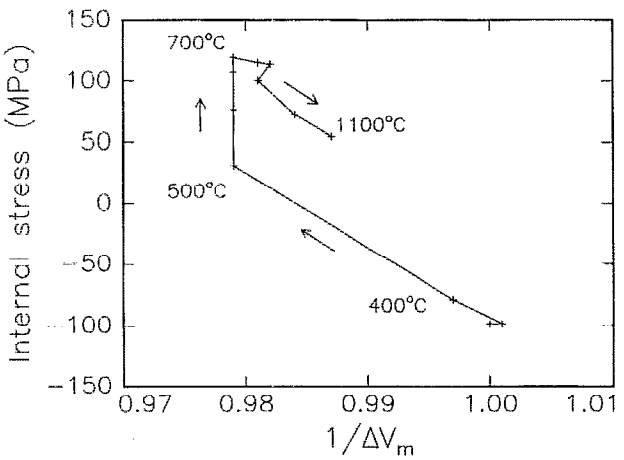

FIG. 8. Internal stress as function of fractional volume for buffer glass (type-I) deposited with a power density of 0.5 W/cm^2.

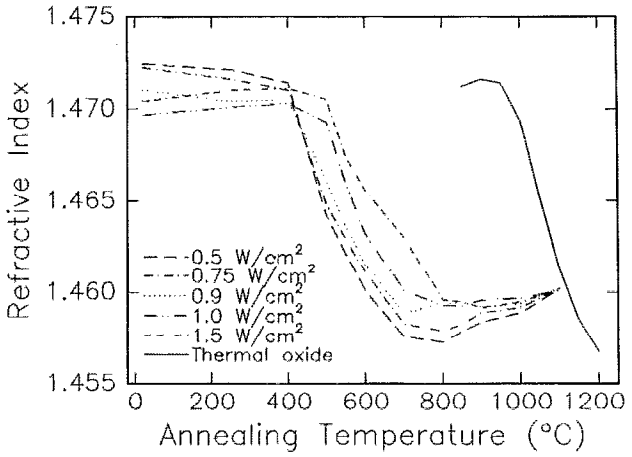

FIG. 9. Refractive index as function of annealing temperature for buffer glass (type-I) deposited at various power densities. The solid line shows the annealing behavior of a dry thermal oxide oxidized at 850 °C.

thermal oxide line. This indicates that a cross-linkage of the glass network is taking place. A cross-linkage of the glass matrix results in an increase in the density of Si–O and Si–N bonds and hereby an increase in the refractive index as obtained from Section III C.

The internal stress of the film is shown in Fig. 8 as function of the relative molar volume. As can be observed, the material relaxes an internal compressive stress for annealing temperatures below 500 °C. At temperatures between 500 °C and 700 °C, the internal stress is increasing in tension. This indicates a release of atoms from the glass matrix. A further increase in anneal temperature is followed by a densification of the material and a relaxation of the internal tensile stress. The motion along the thermal oxide line as function of annealing temperature suggests that a release of internal tension will result in a motion up the line, whereas a release of internal compression will result in a motion down the line.

The effective dielectric constants and internal stress for material deposited at higher power densities behave in a similar way. The thickness change upon anneal is, however, reduced with increasing power density and the nitrogen is released at slightly higher annealing temperatures. This is in accordance with the lower nitrogen and hydrogen concentrations of the PECVD deposited material.

In contrast to the buffer glass, the thickness of the core glass decreases upon annealing. The densification follows, however, the same slope in the Clausius–Mossotti analysis as for the buffer glass. A smaller decrease in thickness is obtained with increasing power density at the expense of a lower nitrogen concentration.

C. Refractive index

The refractive index as function of annealing temperature is shown in Figure 9, for the samples deposited with various power densities. Along with the measured refractive index, the annealing behavior of a dry thermal oxide oxidized at 850 °C is shown.[15]

The refractive index of all deposited samples is in the range from 1.4705 to 1.4720. The refractive index is constant up to an annealing temperature of ~400 °C. A decrease in refractive index is observed for annealing temperatures in the range from 400 °C to 800 °C. Annealing at temperatures above 800 °C leads to an increase in the refractive index. The refractive index value at 1100 °C can be observed to approach the refractive index of the thermal oxide.

From the slopes of the oxide lines in Figure 7 the refractive index dependence on the material density change can be determined. With the refractive index table value of silica glass[25] and corresponding density[26] the dependence of the refractive index (632.8 nm) on the material density for silicon oxy-nitride is estimated to be

$$n(\rho) = 1.4585 + 0.2285(\rho - 2.21). \tag{7}$$

The refractive index of silicon oxy-nitride for material with a nitrogen concentration below 30 at. % can be described by the density Equation (7) as shown in Section III C.

With a refractive index in the 1.4705-1.4720 range the material is deposited in a densified state, with a material density of 2.26–2.27 g/cm^3. The shift in effective dielectric constant for the 0.5 W/cm^2 buffer glass at annealing temperatures between 500 °C and 700 °C corresponds to a decrease in density of 0.029 g/cm^3. The decrease in the effective dielectric constant is observed for a constant volume, which makes it possible to determine the reduction in nitrogen concentration. The density decrease corresponds to a decrease in the nitrogen concentration of $1.2 \cdot 10^{21}$ cm^{-3}. This is in fairly good agreement with the reduction in concentration of $1.3 \cdot 10^{21}$ cm^{-3} determined by the SIMS analysis.

The estimated densities of deposited material are in accordance with the findings of Devine.[27] For a similar deposition system and gas mixture, a mass density of 2.30 $\pm$0.04 g/cm^3 is determined. A thermal anneal at 950 °C reduces the material density by 0.05 g/cm^3. The observation by Devine of positive charge defect centers which only are activated once the film has been annealed can be taken as an

indication for the release of nitrogen. Similar behavior is reported on by Fitch *et al.*[15] Here an increase in the interface state defect density of MOS capacitors is observed. The highest increase in defect density is observed for material annealed at 600 °C and decreasing with increasing anneal temperature. The high defect concentration at 600 °C can be associated with the release of nitrogen. The decrease observed for higher annealing temperatures might be due to an increased cross-linkage of the material.

V. CONCLUSION

It is shown that the PECVD process follows the normal valence selection rules during the deposition process. Deviations from the stoichiometric composition is due to the presence of hydrogen in the source gases, which is included in the glass matrix during deposition.

The refractive index (at 632.8 nm) of oxy-nitride is found to be determined by the mass density of the material for Si–N bond concentrations below 0.4. The presence of nitrogen accommodates more sites for silicon, which causes the material density, and hereby the electron concentration (refractive index), to increase.

It is suggested that the relative oxygen concentration in the gas flow is the major deposition characterization parameter, and that water vapor is the predominant reaction byproduct. A model, that combine the chemical net reaction and the stoichiometric rules, is found to agree with measured deposition rates for given material compositions.

It is observed that PECVD silicon oxy-nitride releases nitrogen and hydrogen at annealing temperatures in the 500 °C–700 °C range. It is suggested that only NH is released from the material upon annealing.

The post anneal hydrogen concentration for the hydrogenated silicon oxy-nitride depends on the deposition power density. Both the nitrogen and hydrogen concentrations decreases with increasing power density. For the core glass, a shift in the nitrogen activation is observed at a power density of 1.0 W/cm^2. At higher power densities the material approaches the nitrogen and hydrogen concentrations of buffer glass and exhibits a similar annealing behavior. For core glass with low power density a higher nitrogen concentration is present of which only a part has bonds to hydrogen. This results in a much smaller reduction in the nitrogen and hydrogen concentrations upon annealing.

The relaxation process taking place during annealing is governed by a viscoelastic relaxation process similar to the relaxation process observed for thermally grown SiO_2. The PECVD material is upon nitrogen release in a state of internal tension. The viscoelastic relaxation process for temperatures above 700 °C is dominated by the relaxation of this internal tension. The relaxation is observed as an increase in the molar volume. The relaxation process for thermal grown oxide is similar. Due to an internal compressive stress the relaxation of the internal stress does, however, lead to a decrease in the molar volume. Both types of material are observed to show a constant molar refraction.

From the constancy of molar refraction a linear relation between the refractive index and material density is determined. This relation is found to be valid for silicon oxy-nitride with a nitrogen concentration below 30 at. %.

ACKNOWLEDGMENTS

The author acknowledges the assistance of P. Shi (MIC, Technical University of Denmark) with the SIMS measurements. This work was supported by the Danish Research Academy.

[1] C. M. M. Denisse, K. Z. Troost, J. B. Oude Elferink, F. H. P. M. Habraken, W. F. van der Weg, and M. Hendriks, J. Appl. Phys. **60**, 2536 (1986).
[2] S. V. Hattangady, R. G. Alley, G. G. Fountain, R. J. Markunas, G. Lucovsky, and D. Temple, J. Appl. Phys. **73**, 7635 (1993).
[3] W. A. P. Claassen, H. A. J. Th.v.d. Pol, A. H. Goemans, and A. E. T. Kuiper, J. Electrochem. Soc. **133**, 1458 (1986).
[4] W. R. Knolle, J. W. Osenbach, and A. Elia, J. Electrochem. Soc. **139**, 3310 (1992).
[5] F. Plais, B. Agius, F. Abel, J. Siejka, M. Puech, G. Ravel, P. Alnot, and N. Proust, J. Electrochem. Soc. **139**, 1489 (1992).
[6] C. H. Henry, R. F. Kazarinow, H. J. Lee, K. J. Orlowsky, and L. E. Katz, Appl. Opt. **26**, 2621 (1987).
[7] F. Bruno, M. delGuidice, R. Recca, and F. Testa, Appl. Opt. **30**, 4560 (1991).
[8] Q. Lai, J. S. Gu, M. K. Smit, J. Schmid, and H. Melchior, Electron. Lett. **28**, 1000 (1992).
[9] V. S. Nguyen, W. A. Lanford, and A. L. Rieger, J. Electrochem. Soc. **133**, 970 (1986).
[10] H. J. Stein, V. A. Wells, and R. E. Hampy, J. Electrochem. Soc. **126**, 1750 (1979).
[11] G. Lucovsky, J. T. Fitch, D. V. Tsu, and S. S. Kim, J. Vac. Sci. Technol. A **7**, 1136 (1989).
[12] H.-J. Schliwinski, U. Schnakenberg, W. Windbracke, H. Neff, and P. Lange, J. Electrochem. Soc. **139**, 1730 (1992).
[13] C. M. M. Denisse, K. Z. Troost, F. H. P. M. Habraken, W. F.v.d. Weg, and M. Hendriks, J. Appl. Phys. **60**, 2543 (1986).
[14] P. Ambree, F. Kreller, R. Wolf, and K. Wandel, J. Vac. Sci. Technol. B **11**, 614 (1993).
[15] J. T. Fitch, S. S. Kim, and G. Lucovsky, J. Vac. Sci. Technol. A **8**, 1871 (1990).
[16] H. J. Stein, Appl. Phys. Lett. **32**, 379 (1978).
[17] G. Smolinsky and T. P. H. F. Wendling, J. Electrochem. Soc. **132**, 950 (1985).
[18] R. E. Newnham, in *Phase Diagrams*, edited by A. M. Alper (Academic, New York, 1978), Vol. 5, pp. 2–71.
[19] H.-O. Mulfinger, J. Am. Ceram. Soc. **49**, 462 (1966).
[20] R. C. Budhani, S. Prakash, H. J. Doerr, and R. F. Bunshah, J. Vac. Sci. Technol. A **5**, 1644 (1987).
[21] S. Hampshire, R. A. L. Drew, and K. H. Jack, Phys. Chem. Glasses **26**, 182 (1985).
[22] J. A. Theil, D. V. Tsu, M. W. Watkins, S. S. Kim, and G. Lucovsky, J. Vac. Sci. Technol. A **8**, 1374 (1990).
[23] D. L. Smith and A. S. Alimonda, J. Electrochem. Soc. **140**, 1496 (1993).
[24] M. Maeda and Y. Arita, J. Appl. Phys. **53**, 6852 (1982).
[25] I. H. Malitson, J. Opt. Soc. Am. **55**, 1205 (1965).
[26] I. Fanderlik, *Silica Glass and Its Application* (Elsevier, Amsterdam, 1991).
[27] R. A. B. Devine, J. Appl. Phys. **66**, 4702 (1989).